2021 18th International Conference on Electrical Engineering, Computing Science and Automatic Control (CCE). Mexico City, Mexico. November 10-12, 2021.

Toward a single-pixel near-infrared low-resolution 2D image reconstruction strategy

C. Osorio Quero[1], A. Manjarrés García[1], D. Durini[1], J. Rangel-Magdaleno[1], J. Martinez-Carranza[2], and R. Ramos-Garcia[3]

[1] *Electronics Department*, [2] *Computer Science Department*, [3] *Optics Department*

Instituto Nacional de Astrofísica, Óptica y Electrónica. (INAOE)

Luis Enrique Erro 1, 72840 Tonantzintla, Puebla, Mexico

email:{caoq, manjarres, ddurini, jrangel, carranza, rgarcia}@inaoep.mx

***Abstract*—In this article, we propose a method to be used for the reconstruction of single-pixel near-infrared (SPI-NIR) low-resolution 2D images using active illumination with a peak wavelength on 1550 nm, that is based on Batch Orthogonal Matching (Batch-OMP) processing algorithms and a region definition in the projection sequence of Hadamard illumination patterns using the Genetic algorithm (GA). Different methods to generate Hadamard pattern sequences have been reported, mostly based on switching the illumination sequence on and off to improve the quality of the reconstructed image, thereby increasing the Structural Similarity Index Measure (SSIM) level and reducing the processing time.These methods are efficient for image sizes of $> 64x64$ virtual pixels,but for lower resolutions with small coherence areas A_{ch}, the SNR level of the reconstructed image is very low, which makes other methods, such as those using the Zig-Zag or Hilbert filling curves for the scanning path, an option for the reconstruction of SPI-NIR low-resolution images.Due to the fact that in the present application, we deal with low-resolution (size image 8 x 4 virtual pixels) SPI-NIR images, we present a solution to improve the obtained image quality (aiming at PSNR$> 10dB$ and SSIM> 0.5) that is based on the use of a specific scanning path and a combination of a genetic algorithm to define the switching sequences of the Hadamard patterns, using Batch-OMP algorithm for image reconstruction, in the processing time range between 20 and 35 ms.**

I. Introduction

This work aims at presenting a strategy for single-pixel image reconstruction based on generation of Hadamard illumination patterns through region definition defined by applying Genetic Algorithms (GA). The latter is used to define the best suiting illumination patterns, as well as the minimum required number of those and the sequence in which they are projected, required to improve the quality of the reconstructed single-pixel images using near infra-red (SPI-NIR) active illumination, in background noise conditions. The latter focuses on applications in Unmanned Aerial Vehicles (UAVs), especially in what their autonomous navigation is concerned. The most common approach for single-pixel imaging (SPI) systems is using the Hadamard illumination patterns [1], mostly preferred over other types of patterns, such as those generated at random [2], or those generated using chaos-based methods [3]. The Hadamard approach defines a sequence of orthogonal and binary illumination patterns that can be created by a digital micromirror device (DMD) or a LED matrix.However, Hadamard patterns do not yield a uniform energy distribution. If we want to reconstruct an SPI image [4] using the Hadamard illumination patterns, considering the order of the final virtual image having "N" virtual pixels in one line and "M" virtual pixels in one row, we would need a sequence of N x M patterns (i.e., for a reconstruction of an image of 64 x 64 virtual pixels, we need to project 4096 different illumination patterns). In practice, for an application where the reconstruction time is a critical factor, as for example it is the case in visual sensing in drones or unmanned vehicles in general, it is not time efficient to project all the required illumination patterns sequentially. Instead, if we desire to reduce the amount of illumination patterns to improve the processing (and pattern projection) time and simultaneously maintain the quality of the reconstructed single-pixel image (with PSNR $> 10dB$ and SSIM > 0.5), we propose using only about 10 % of the originally required patterns by applying the Nyquist principle [5] and the compressing sensing (CS) techniques [6]. For an SPI-NIR vision system of low-resolution yielding images with only 8 x 4 virtual pixels, if we consider the Nyquist principle for determining the amount of minimum required samples [5], to achieve a compression factor of 10%, at the theoretical level, we would need to project only six patterns to reconstruct a 2D image of mentioned characteristics.Nevertheless, it results impossible to accurately emulate this condition in practice, mainly due to background noise and reflection and absorption characteristics of the objects in the scene being depicted. Beacuse will be need to increase the number of patterns to be able to detect low-level details of 2D image reconstructed. There are some techniques that operate over the Hadamard matrix manipulating the illumination sequece, without need to increasing the numbers of patters , such as Russian Doll [7] technique , the Origami Pattern [8], and cake-cutting [9], that improve the quality of 2D reconstrution. Taking into account all the previously described methods, we propose developing a projection sequence of areas A_p, that changes the on/off state of the patterns through a genetic algorithm [10]. To be able to define the A_p areas that will be modified, we must define a fitness function that considers the set goals of single-pixel image reconstruction times $< 30ms$ and SSIM > 0.5. To evaluate the performance of the projection areas, we will use some scanning methods such as Zig-Zag [11], Spiral [12], or

978-1-6654-0029-9/21/$31.00 ©2021 IEEE

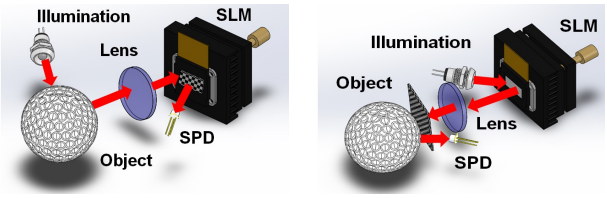

(a) (b)

Fig. 1: Two different approaches applied to SPI: a) Front modulation: the object illuminated by a light source and the light reflected by it gets directed through a lens onto an SLM,where is capture by the SPD, b) Back modulation: the SLM device project a sequence of patterns and reflected light is capture by the SPD [1].

Hilbert path [13] adapted to the Hadamard projection sequence to reconstruct 8 x 4 virtual pixel images. As reconstruction algorithms, we will use the Compressive Sensing (CS) algorithm Batch-OMP [14] to determine our method's performance under different background noise conditions.

Integrating NIR vision systems into UAVs offers higher detection capabilities under low visibility or rainy or foggy weather conditions, if compared to the classic performance of traditional RGB sensor based cameras operating in the visible (VIS) part of the spectra in the wavelength range between 400 and 800 nm. In this work, we present a proof of concept of an SPI-NIR low-resolution imaging system based on a Hadamard on-off firing projection strategy illumination sequence, using GA to improve the quality of the reconstructed 2D images. With this approach, we aim at additionally increasing the robustness of our SPI-NIR system in outdoor conditions for UAV applications.

II. SINGLE-PIXEL OBJECT RECONSTRUCTION

The generation of single-pixel images is based on the reconstruction of the spatial information embedded in the output signals produced by a single pixel detector (SPD) in response to a sequence of structured illumination patterns created using SLM, DMD, or other similar active illumination technologies. There are two types of configurations that can be used in SPI. Namely, the structured illumination scheme termed front modulation (see Fig.1a), and a structured detection scheme termed back modulation (see Fig. 1b).

The relationship between the structured and reflected light signal measurement can be expressed using Eq. (1) [1].

$$S_i = \alpha \sum_{x=1}^{M} \sum_{y=1}^{N} O\left(x,y\right) \Phi_i\left(x,y\right) \tag{1}$$

In Eq. (1), (x, y) are the spatial coordinates, O denotes the measured output signal of the used SPD, considering additionally the SPD and the depicted object reflectivities (see Fig.1) , Φ_i is i_{th} structured pattern of size M x N, S_i is the i_{th} single-pixel measurement corresponding to Φ_i, and α is a constant factor defined by the opto-electronic response of the used SPD. From the previously defined sequence of structured illumination patterns projected onto the scene, and the measured SPD output signals generated in response to each of those projected illumination patterns, if compressive sensing (CS) algorithms such as as Batch-OMP [14] are applied, the single-pixel image $I(x, y)$ can be reconstructed. The reconstructed image $I(x, y)$ can be defined as the inner product of S_i, the measured output signal generated by the SPD, and the structured illumination pattern $\Phi_i(x, y)$ used to produce said response, additionally proportional to the measured object reflectivity O [1], as expressed in Eq. (2).

$$I\left(x,y\right) = \alpha \sum_{x=1}^{M} \sum_{y=1}^{N} S_i \Phi_i\left(x,y\right) \tag{2}$$

A. Generation of the Hadamard sequence of patterns

To generate the Hadamard sequence of patterns, firstly, we need to define a square matrix H, defined by the Eq. (3), where its components are +1 or -1 with two distinct rows that coincide in exactly n/2 positions, and must satisfy the condition $HH^T = nI$. For N orders of the H matrix, we use the Kronecker product, also defined in Eq. (3), where 2^k is an integer with k > 0, and the size of the H matrix is M x N (the example matrix where M = N, is presented in the Eq. (4)) [4], with m = 1, 2, 3,..., M, and n = 1, 2, 3,..., N. From the H matrix defined, we can construct the Hadamard sequence using the Sylvester's recursive matrix generation principle defined by Eq. (2) to obtain the Hadamard matrix $H_{2^k}(m, n)$.

$$H_{2^k} = \begin{bmatrix} H_{2^{k-1}} & H_{2^{k-1}} \\ H_{2^{k-1}} & -H_{2^{k-1}} \end{bmatrix} = H_2 \otimes H_{2^{k-1}} \tag{3}$$

$$H_{2^k} = \begin{bmatrix} H\left(1,1\right) & H\left(1,2\right) & ... & H\left(1,N\right) \\ H\left(2,1\right) & H\left(2,2\right) & ... & H\left(2,N\right) \\ ... & ... & ... & ... \\ H\left(M,1\right) & H\left(M,2\right) & ... & H\left(M,N\right) \end{bmatrix} \tag{4}$$

The Hadamard based sequence of projections presents some limitations, mainly due to the fact that the coefficients of the Hadamard matrix do not present a uniform energy distribution. Moreover, its energy packing efficiency (EPE) is also low [14], which decreases the quality of the reconstructed image when using only a few samples together with CS image reconstruction algorithms. A proposed solution to improve the quality of the image reconstruction is to apply different types of projection sequences, based, for example, on the Zig-Zag [11], Spiral [12], or Hilbert [13] space filling curves (see Fig.2). These methods provide the best EPE relation, increasing the quality of the reconstructed images.

III. REGION DEFINITION FOR PROJECTION OF ILLUMINATION PATTERNS

To define the projection areas A_p, we start by dividing all the Hadamard N x N projection patterns required (for our application, the maximum required number of patterns is 64) into groups of N / 4, each containing a number of N / 16 patterns (see Fig.3a). These groups will be defined as A_p projection areas and represented as a matrix H_p defined by Eq. (5).

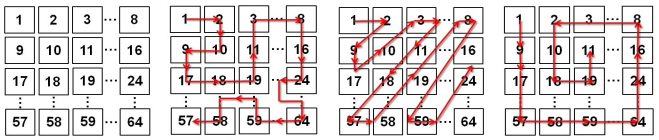

(a) (b) (c) (d)

Fig. 2: Hadamard H_{64} scanning scheme, a) basic Hadamard sequence, b) Hilbert scan [13], c) Zig-Zag scan [11], d) Spiral scan [12].

$$H_p = \begin{bmatrix} A_{p_1} & A_{p_2} & A_{p_3} & A_{p_4} \\ A_{p_5} & A_{p_6} & A_{p_7} & A_{p_8} \\ A_{p_9} & A_{p_{10}} & A_{p_{11}} & A_{p_{12}} \\ A_{p_{13}} & A_{p_{14}} & A_{p_{15}} & A_{p_{16}} \end{bmatrix} \quad (5)$$

The matrix H_p is optimized to increase the quality of the reconstructed image while maintaining the processing time required $< 30ms$, using the number of used Hadamard patterns between 20 and 80%. As an optimization strategy, a genetic algorithm method (GA) [15] can be applied, in which the elements of the H_p matrix are encoded to form a binary vector (forming the GA initial population vector), where the "1" elements define the groups without a change throughout the Hadamard sequence of patterns, and "0" elements represent the groups of matrix elements that do undergo a change throughput the sequence of Hadamard patterns, being sequentially switched "on" and "off".

A. Definition of the most optimum projection of Hadamard patterns using illumination regions defined by the GA algorithm

To determine the most optimal sequence of Hadamard patterns to be projected in order to obtain the highest possible quality of the reconstructed images, as defined by the application of figures of merit PSNR $> 10dB$ and SSIM > 0.5, it is necessary to define which projection sequences are necessary to be inverted to comply with our goal. To do this, GA was used to determine the most optimal "on" and "off" conditions of the different Hadamard matrix elements throughout the different pattern sequences in an evolutionary way. We used our data-set formed with images of spherical and square objects, using 8 x 4 pixel image sizes for test. Initially, we defined a Hadamard projection sequence of 64 patterns divided into 16 groups (see Fig.3b) containing four elements of the projection sequence (see Algorithm 1, input elements). These elements were used to form the vector V_p that contains the matrix elements positions encoded in a binary form, and its dimensions are of 1 x 16. For the GA based evaluation process used, it was necessary to define an initial population of N = 8, divided into six parents. This initial population is an 8 x 16 pixel matrix containing random data (see Algorithm 1, line 2). For the evaluation of the projection sequences, a fitness function was defined, which will receive the V_p vector containing the positions of the different Hadamard matrix elements throughout the sequence of generated patterns, that

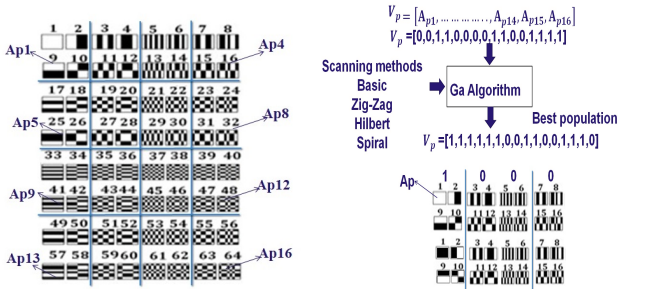

(a) (b)

Fig. 3: Sequence area generation A_p using GA algorithm, a) Hadamard projection sequence of 64 patterns divided into 16 groups containing four elements of the projection sequence, area projection A_p. b) GA Algorithm that evaluates the different sequence switching on-off sequence in the Hadamard projection using the vector V_p with position binary of the groups.

correspond to the population to be evaluated (see Algorithm 1, line 4). We used the Zig-Zag [11], Hilbert [13], and Spiral [12] scanning sequences in a comparative study for the reconstruction of the single-pixel image of interest.

The fitness function used performs image reconstruction using Batch-OMP algorithms, and it evaluates the best projection sequence calculated, considering the levels of SSIM and PSNR projected [16], as well as the processing time required for image reconstruction. This process is iterative, setting the maximum number of generations to 100 (see Algorithm 1, line 3). Every 16 generations, a mutation takes place in order to find a new population (see Algorithm 1, line 6-7). Once the iterative process finishes, the algorithm calculates the fitness of the best suited population (see Agorithm 1, line 10), which determines the best vector V_p obtained containing the exact positions of the areas A_p that must be inverted in the "on"-"off" switching sequence in the Hadamard projection (see Algorithm 1, line 11), as shown in Fig.3b.

IV. EVALUATION OF THE METHOD PROPOSED USING HADAMARD REGION-PROJECTIONS CALCULATED BY THE GA ALGORITHM

To evaluate the performance of the proposed Hadamard region-projection method, where the projected regions are calculated using the GA algorithm, we reconstructed an SPI-NIR 2D image of a square object (see Fig.5b), and another one of a sphere (see Fig.5a), using the Batch-OMP algorithm to process the data measured in an environment with controlled illumination (see Fig.4a) at a distance of 18 cm from the photodetector. For the latter, we additionally carried out a comparative study between the images reconstructed using the Hadamard region-projection method on the one side, and unmodified Hadamard patterns on the other. In both cases,we used different scanning sequences using the Basic, Zig-Zag [11], Hilbert [13], and Spiral [12] approaches, respectively, adding each time different levels of background illumination (see Fig.4b) in order to simulate different outdoor conditions: very-cloudy (5 KLux), half-cloudy (15 KLux), midday (30

Algorithm 1: Regions-projection Hadamard GA algorithm [15]:

Function RegionProjection (A_p, I, S_m, n_g) :
Input : A population vector A_p is defined, image I and scanning Basic, Zig-Zag, Hilbert or Spiral S_m, number of generation n_g
Output: On-off switching sequence optimized of Hadamard
Initialization: Population *pop* matrix 8x16
for $it = 1 \ \ to \ \ n_g$ **do**
    fitnessGA= fitness (pop, S_m)
    parents = poolGA(pop, fitnessGA)
    offspringC = crossover(parents)
    offspringM = mutationGA(offspringC)
    pop = [parents, offspringM]
end
fitnessGA= fitness (pop, S_m) contains the vector sequence of switch on-off area A_p sequence Hadamard
On-off switching sequence in the Hadamard projection
return

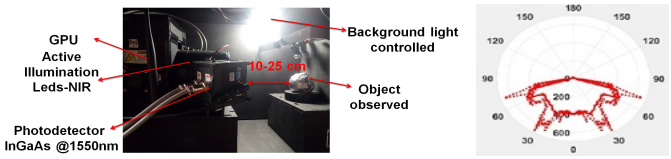

(a) (b)

Fig. 4: Experimental setup to vision system SPI-NIR with active illumination in the wavelength 1550 nm at configuration back modulation (see Fig.1b),a) testing bench with controlled illumination background range of intensity between 0 to 50 KLux, b)polar intensity diagram of source light of the type semi-direct used for the testing bench.

KLux), and clean-sky (40-50 Lux). In order to evaluate the capabilities of each method pursued, we compared the obtained levels of PSNR, SSIM, as well as the processing time required in each image reconstruction.

For the condition of Hadamard region-projection, the following areas were defined for the case of spherical type surfaces in terms of the projection sequences: V_p= [1, 1, 1, 1, 1, 0, 0, 1, 1, 0, 0, 1, 1, 1, 0], scanning Zig-Zag V_p = [0, 0, 0, 0, 1, 0, 1, 0, 0, 0, 0, 0, 0, 1, 1, 0], scanning Hilbert V_p = [1, 1, 0, 1, 1, 0, 0, 0, 1, 0, 0, 1, 1, 1, 0, 0] and scanning Spiral V_p = [1, 0, 0, 0, 0, 0, 0, 0, 1, 0, 0, 0, 0, 0, 0,].For the case of square type surfaces, projection sequences V_p=[1, 1, 0, 1, 0, 1, 0, 0, 1, 0, 0, 1, 0, 1, 1, 0], Zig-Zag scanning V_p = [0, 0, 0, 0, 1, 0, 1, 0, 0, 0, 0, 0, 0, 1, 1, 0], Hilbert scanning V_p = [1, 1, 0, 1, 1, 0, 0, 0, 1, 0, 0, 1, 1, 1, 0, 0], and Spiral scanning V_p = [1, 0, 0, 0, 0, 0, 0, 0, 1, 0, 0, 0, 0, 0, 0, 0].

A. Discussion: Method of Hadamard region-projections calculated using the GA algorithm

During the performed tests, we could observe that for spherical surfaces (see Fig. 5b) in outdoor conditions with background illumination levels between 20 and 40 Klux, if Zig-Zag and Spiral surface filling curves (SFC) were respectively used, the reconstructed images presented a PSNR (28 dB) higher than when other scanning methods were used (see Fig. 8c,d), yielding an SSIM between 0.6 to 0.68 (see Fig. 6c,d). The images reconstructed using the Hilbert scanning curve and the basic projection sequence, respectively, yielded under the same measuring conditions an SSIM range between 0.58 and 0.65 and a very similar PSNR (27 - 28 dB). The measurements using the unmodified patterns method showed an SSIM range between 0.5 and 0.56 (see Fig. 6a,b) for PSNR = 27 dB. The measurements performed using the Zig-Zag (see Fig. 6c) and Spiral (see Fig.6d) SFCs, respectively, present changes in the "on"-"off" sequence of 12 and 13 A_p areas, if compared to the basic scanning (with 5 A_p areas) and the Hilbert scanning approach (with 8 A_p areas), respectively. These last two scanning methods present more high-frequency information with a processing time between 28 and 29 ms (see Table.II), with an improving rate of time 11% (6) for the Spiral scan . When the same experiments were performed depicting square surfaces (see Fig. 5a), we observed that the Hadamard region projection method presented a higher image reconstruction efficiency with reconstruction times of around 28 ms for the basic, Hilbert, and Zig-Zag scanning methods (see Table. I), with an improving rate of time 18%(6) for the Zig-Zag scan . More significant changes in the projection areas were observed here, if compared with the same measurements performed using spherical surfaces. In both cases, eight A_p areas were defined for the basic projection sequence and the Hilbert curve based method, 12 A_p areas for the Zig-Zag approach, and 14 A_p areas using the Spiral curve. The Hilbert scanning method maintained an SSIM level oscillating between 0.86 and 0.89 (see Fig.7b) with a PSNR level between 30 to 29 dB (see Fig.7b). For the case where Hadamard region-projections were used, calculated through the GA, the SSIM level yielded was situated between 0.8 and 0.86 (see Fig.7b) with a PSNR level between 28.7 and 28.2 dB (see Fig.7b). Therefore, this scanning method results being more robust if compared to the other scanning methods proposed, such as the Basic, Zig-Zag, and Spiral methods, respectively (for SSIM values, see Fig. 7a,c,d, and for PSNR see Fig. 9a,c,d).

TABLE I: SPI-NIR 2D image reconstruction time with unmodified patterns method and region-projection Hadamard GA for cube object

Pattern	Time$_{withoutGA}(ms)$	Time$_{GA}(ms)$	Improvement rate (%)
Basic	30.6	28.49	6.89
Hilbert	31.73	27.7	12.7
Zig-Zag	34.42	27.93	18.85
Spiral	28.38	27.79	2

V. PROPOSED REGION-PROJECTION METHOD APPLIED TO SINGLE-PIXEL UAV APPLICATIONS

The atmosphere's capacity to absorb radiation in the wavelength range belonging to the near-infrared (NIR) part of the

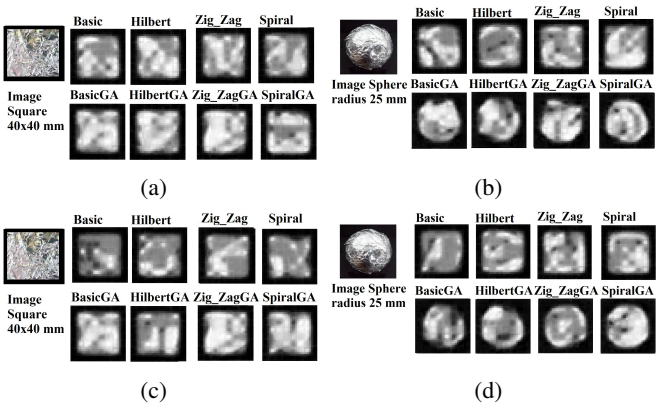

Fig. 5: 2D SPI-NIR Image reconstructed size 8x4 in static condition with modified patterns method and region-projection Hadamard GA algorithm at a distance of 18 cm of the photodetector using basic scan, Hilbert scan, Zig-Zag scan, and Spiral scan. Square object intensity light background: a) 5KLux , c) 40KLux . Sphere object intensity light background: b) 5KLux , d) 40KLux.

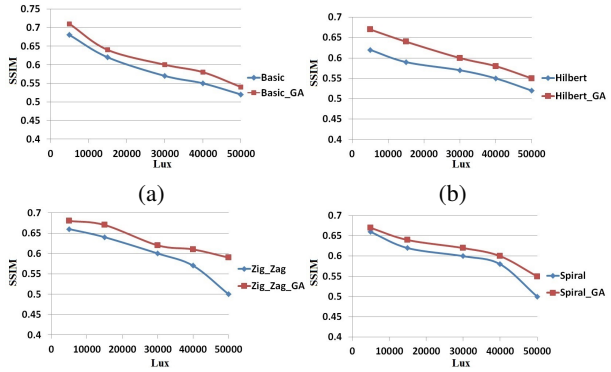

Fig. 6: SSIM level of reconstructed SPI-NIR 2D image spherical surface with unmodified patterns method (blue line) and region-projection Hadamard GA algorithm (red line) at distance at 18 cm of the photodetector: a) Basic scan, b) Hilbert scan, c) Zig-Zag scan, d) Spiral scan.

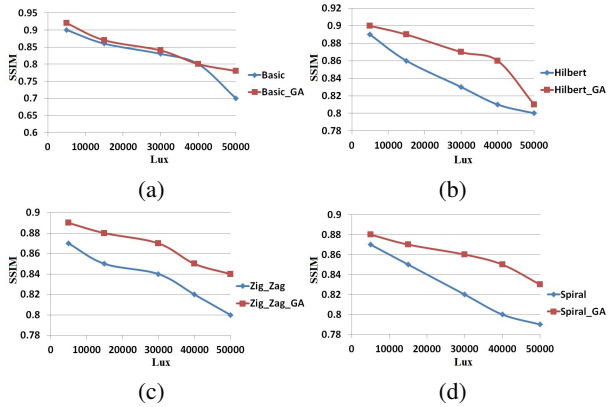

Fig. 7: SSIM level of reconstructed SPI-NIR 2D image square surface with unmodified patterns method (blue line) and region-projection Hadamard GA algorithm (red line) at distance at 18 cm of the photodetector: a) Basic scan, b) Hilbert scan, c) Zig-Zag scan, d) Spiral scan.

TABLE II: SPI-NIR 2D image reconstruction time with unmodified patterns method and region-projection Hadamard GA for sphere object

Pattern	Time$_{withoutGA}(ms)$	Time$_{GA}(ms)$	Improvement rate (%)
Basic	29.89	27.5	8
Hilbert	29.14	27.1	12.7
Zig-Zag	30.03	27.2	9.7
Spiral	30.7	27.8	11

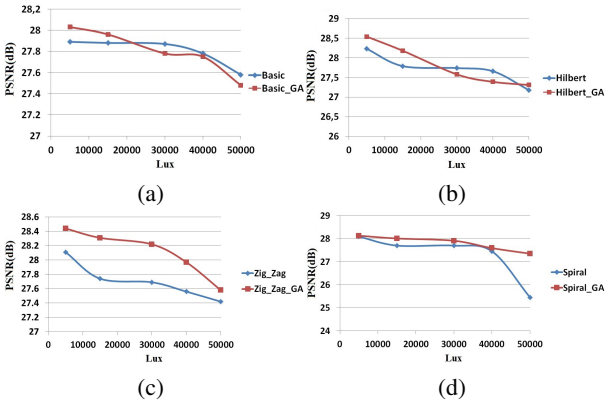

Fig. 8: PSNR level of reconstructed SPI-NIR 2D image spherical surface with unmodified patterns method (blue line) and region-projection Hadamard GA algorithm (red line) at distance at 18 cm of the photodetector: a) Basic scan, b) Hilbert scan, c) Zig-Zag scan, d) Spiral scan.

spectra is the best option for generating single-pixel (or line-sensor-based) images based on NIR active illumination for unmanned systems, as this phenomena reduces the amount of background illumination present in the illumination wavelength range of interest thus reducing also the amount of noise present in the system. Throughout the last decades, a continuous improvement of single-pixel image reconstruction algorithms has been taking place, aiming at processing times

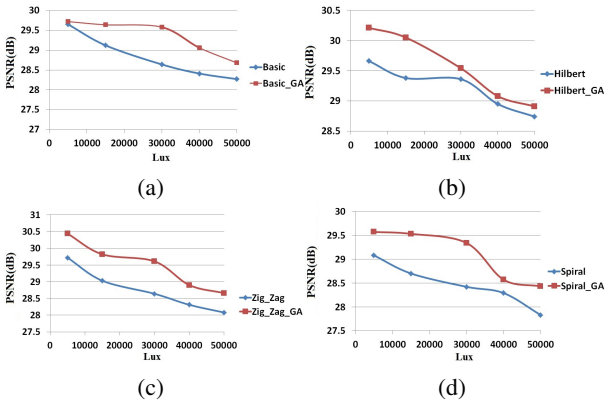

Fig. 9: PSNR level of reconstructed SPI-NIR 2D image square surface with unmodified patterns method (blue line) and region-projection Hadamard GA algorithm (red line) at distance at 18 cm of the photodetector: a) Basic scan, b) Hilbert scan, c) Zig-Zag scan, d) Spiral scan.

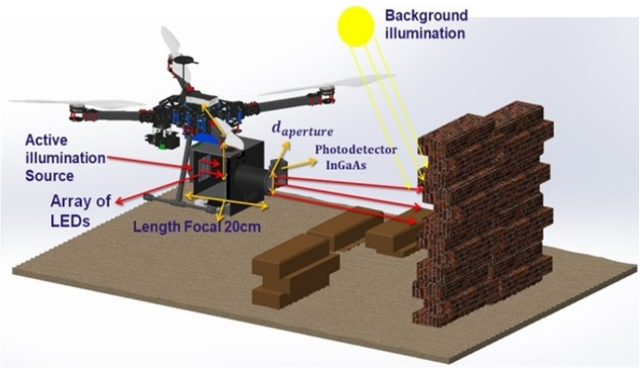

Fig. 10: Schematic view to illustrate a single-pixel NIR vision system carried by a drone [14].

short enough to allow for near real-time image processing and thus enabling autonomous navigation. If decision making depends on the information to be extracted from reconstructed single pixel images, the system response times acquire a paramount importance. For this type of applications, having a high resolution of images of the environment presents a high limitation in the vehicle's response time, so reducing the size to an 8 x 4 pixel image resolution is a possible way to address this issue. Although this approach limits the quality of the reconstructed images, developing techniques that can improve the SSIM level of the reconstructed image in a processing time $< 30ms$ allows to increase the single-pixel vision system's capabilities for UAV applications (see Fig. 10).

$$improvement_{time\%} = \frac{(Time_{withoutGA} - Time_{GA})}{Time_{withoutGA}} x100 \tag{6}$$

VI. CONCLUSION

In this paper, we presented a method for generating Hadamard patterns based on the Hadamard region projection method using the GA to define these regions of interest. In order to improve the quality of the reconstructed single-pixel images carried out by the SPI-NIR system proposed, with potential applications for UAV navigation, our proposed Hadamard region projection method yielded an acceptable performance. The 8 x 4 pixel single-pixel images obtained with this method had an SSIM > 0.6 and a PSNR$> 28dB$, respectively, that could be compared with the Hadamard unmodified patterns method yielding an SSIM < 0.6 and PSNR$< 25dB$ that required almost 3 ms more processing time.We depicted in our experiments objects with sphere and square surfaces, respectively, using different scanning curves, namely the Zig-Zag, the Spiral, and the Hilbert curves, respectively, under controlled background illumination ranging between 20 and 40 Klux. Our results indicate that the Hilbert-based scanning method combined with the Hadamard region projection yield the best performance in the SPI-NIR 2D image reconstruction, if the figures of merit SSIM and PSNR, as well as the image reconstruction processing time(see Table. I,II), are taken into account. The proposed method also proved to be robust enough in background noise conditions. In the evaluation, we fixed the goal to reach a reconstruction time below 30 ms, with Hilbert and Zig-Zag methods being the fastest ones, and the Spiral based one, the slowest. The availability to have processing time $< 30ms$ in single-pixel imaging allows to increase the single-pixel vision system's capabilities with potential applications UAVs.

ACKNOWLEDGMENT

We are thankful for the technical support received from the Laboratory of Illumination and Efficient Energy from INAOE.

REFERENCES

[1] G. M. Gibson, S. D. Johnson, and M. J. Padgett, "Single-pixel imaging 12 years on: a review," *Opt. Express*, vol. 28, no. 19, pp. 28 190–28 208, Sep 2020. [Online]. Available: http://www.opticsexpress.org/abstract.cfm?URI=oe-28-19-28190

[2] Q. Chen, S. K. Chamoli, P. Yin, X. Wang, and X. Xu, "Imaging of hidden object using passive mode single pixel imaging with compressive sensing," *Laser Physics Letters*, vol. 15, no. 12, p. 126201, oct 2018. [Online]. Available: https://doi.org/10.1088/1612-202x/aae216

[3] H. Gan, S. Xiao, T. Zhang, Z. Zhang, J. Li, and Y. Gao, "Chaotic pattern array for single-pixel imaging," *Electronics*, vol. 8, no. 5, 2019. [Online]. Available: https://www.mdpi.com/2079-9292/8/5/536

[4] Z. Zhang, X. Wang, G. Zheng, and J. Zhong, "Hadamard single-pixel imaging versus fourier single-pixel imaging," *Opt. Express*, vol. 25, no. 16, pp. 19 619–19 639, Aug 2017. [Online]. Available: http://www.opticsexpress.org/abstract.cfm?URI=oe-25-16-19619

[5] X. Yu, R. I. Stantchev, F. Yang, and E. Pickwell-MacPherson, "Super sub-nyquist single-pixel imaging by total variation ascending ordering of the hadamard basis," *Scientific Reports*, vol. 10, no. 1, p. 9338, Jun 2020. [Online]. Available: https://doi.org/10.1038/s41598-020-66371-5

[6] M. Elad, "Optimized projections for compressed sensing," *IEEE Transactions on Signal Processing*, vol. 55, no. 12, pp. 5695–5702, 2007.

[7] M.-J. Sun, L.-T. Meng, M. P. Edgar, M. J. Padgett, and N. Radwell, "A russian dolls ordering of the hadamard basis for compressive single-pixel imaging," *Scientific Reports*, vol. 7, no. 1, p. 3464, Jun 2017. [Online]. Available: https://doi.org/10.1038/s41598-017-03725-6

[8] W.-K. Yu and Y.-M. Liu, "Single-pixel imaging with origami pattern construction," *Sensors*, vol. 19, no. 23, 2019. [Online]. Available: https://www.mdpi.com/1424-8220/19/23/5135

[9] W.-K. Yu, "Super sub-nyquist single-pixel imaging by means of cake-cutting hadamard basis sort," *Sensors*, vol. 19, no. 19, 2019. [Online]. Available: https://www.mdpi.com/1424-8220/19/19/4122

[10] S. V. Petoukhov, "The degeneracy of the genetic code and hadamard matrices," 2010.

[11] H. Ma, A. Sang, C. Zhou, X. An, and L. Song, "A zigzag scanning ordering of four-dimensional walsh basis for single-pixel imaging," *Optics Communications*, vol. 443, pp. 69–75, 2019. [Online]. Available: https://www.sciencedirect.com/science/article/pii/S0030401819301506

[12] T. M. Cabreira, C. D. Franco, P. R. Ferreira, and G. C. Buttazzo, "Energy-aware spiral coverage path planning for uav photogrammetric applications," *IEEE Robotics and Automation Letters*, vol. 3, no. 4, pp. 3662–3668, 2018.

[13] U. Ujang, F. Anton, S. Azri, A. Rahman, and D. Mioc, "3d hilbert space filling curves in 3d city modeling for faster spatial queries," *International Journal of 3D Information Modeling (IJ3DIM)*, 04 2014.

[14] C. A. Osorio Quero, D. D. Romero, R. Ramos-Garcia, J. de Jesus Rangel-Magdaleno, and J. Martinez-Carranza, "Towards a 3d vision system based on single-pixel imaging and indirect time-of-flight for drone applications," in *2020 17th International Conference on Electrical Engineering, Computing Science and Automatic Control (CCE)*, 2020, pp. 1–6.

[15] S. Pal, D. Bhandari, and M. Kundu, "Genetic algorithms for optimal image enhancement," *Pattern Recognition Letters*, vol. 15, pp. 261–271, 03 1994.

[16] Z. Wang and A. Bovik, "A universal image quality index," *IEEE Signal Processing Letters*, vol. 9, no. 3, pp. 81–84, 2002.